Manuscript prepared for Clim. Past
with version 2015/04/24 7.83 Copernicus papers of the LaTeX class copernicus.cls.
Date: 18 March 2016

Hosed vs. Unhosed: interruptions of the Atlantic Meridional Overturning in a global coupled model, with and without freshwater forcing

Nicolas Brown[1] and Eric D. Galbraith[1,2,3]

[1]Dept. of Earth and Planetary Science, McGill University, Montreal QC H3A 2A7
[2]Institucio Catalana de Recerca i Estudis Avanats (ICREA), 08010 Barcelona, Spain
[3]Institut de Ciencia i Tecnologia Ambientals (ICTA) and Department of Mathematics, Universitat Autonoma de Barcelona, 08193 Barcelona, Spain

Correspondence to: eric.d.galbraith@gmail.com

Abstract. It is well known that glacial periods were punctuated by abrupt climate changes, with large impacts on air temperature, precipitation, and ocean circulation across the globe. However, the long-held idea that freshwater forcing, caused by massive iceberg discharges, was the driving force behind these changes has been questioned in recent years. This throws into doubt the abundant literature on modelling abrupt climate change through 'hosing' experiments, whereby the Atlantic Meridional Overturning Circulation (AMOC) is interrupted by an injection of freshwater to the North Atlantic: if some, or all, abrupt climate change was not driven by freshwater input, could its character have been very different than the typical hosed experiments? Here, we describe spontaneous, unhosed oscillations in AMOC strength that occur in a global coupled ocean-atmosphere model when integrated within a particular envelope of boundary conditions. We compare these unhosed oscillations to hosed oscillations under a range of boundary conditions in order to examine how the global imprint of AMOC variations depends on whether or not it is the result of external freshwater input. Our comparison includes surface air temperature, precipitation, dissolved oxygen concentrations in the intermediate-depth ocean, and marine export production. The results show that the background climate state has a significant impact on the character of AMOC interruptions, including marked variations in tropical precipitation and in the North Pacific circulation. Despite these differences, the first order response to AMOC interruptions is quite consistent among all simulations, implying that the ocean-sea ice-atmosphere dynamics associated with an AMOC weakening dominate the global response, regardless of whether or not freshwater input is the cause. Notable exceptions lie in the direct impact freshwater inputs can have on the strength of other polar haloclines, particularly the Southern Ocean, to which freshwater can be transported relatively quickly after injection in the North Atlantic.

1 Introduction

'Abrupt' climate changes were initially identified as decadal-centennial temperature changes in Greenland ice deposited during the last ice age (Dansgaard et al., 1984), and subsequently recognized as globally-coherent climate shifts (Voelker, 2002; Alley et al., 2003). Abrupt climate changes were shown to have involved changes in the latitudinal extent and strength of the AMOC (Clark et al., 2002), but also impacted global patterns of precipitation, surface air temperature, ocean biogeochemistry and atmospheric trace gas composition (Behl and Kennett, 1996; Indermühle et al., 2000; Clement and Peterson, 2008; Luthi et al., 2008; Harrison and Sanchez Goñi, 2010; Schmittner and Galbraith, 2008). Abrupt climate changes were associated, in early studies, with layers of ice-rafted detritus that blanketed the North Atlantic during brief intervals of the last ice age (Heinrich, 1988), leading to the idea that recurring pulses of freshwater input had been the cause of AMOC interruptions. As evocatively described by Broecker (1994), armadas of icebergs, periodically discharged from the northern ice sheets to melt across the North Atlantic (MacAyeal, 1993), would have spread a freshwater cap that impeded convection and consequently, through the Stommel (1961) feedback, would have thrown a wrench in the overturning. Inspired by this idea, generations of numerical models have been subjected to freshwater 'hosing' experiments, whereby the sensitivity of the AMOC to varying degrees of freshwater input have been tested, and the responses shown to vary as a function of background climate state and experimental design (Fanning and Weaver, 1997; Ganopolski and Rahmstorf, 2001; Schmittner et al., 2002; Timmermann et al., 2003; Rahmstorf et al., 2005; Stouffer et al., 2006; Krebs and Timmermann, 2007; Hu et al., 2008; Otto-Bliesner and Brady, 2010; Kageyama et al., 2013; Gong et al., 2013; Roberts et al., 2014). Multiple studies have shown a good degree of consistency between aspects of these hosing simulations and the observed global signatures of abrupt climate change (Schmittner et al., 2007b; Liu et al., 2009; Menviel et al., 2014).

However, other model simulations have shown that spontaneous changes in the AMOC can occur in the absence of freshwater inputs (Winton, 1993; Sakai and Peltier, 1997; Hall and Stouffer, 2001; Ganopolski and Rahmstorf, 2002; Schulz, 2002; Loving and Vallis, 2005; Wang and Mysak, 2006; Colin de Verdière, 2007; Friedrich et al., 2010; Arzel et al., 2011; Kim et al., 2012; Drijfhout et al., 2013; Peltier and Vettoretti, 2014; Vettoretti and Peltier, 2015). Although uncommon, these 'unhosed' oscillations show that the AMOC can vary as a result of processes internal to the ocean-atmosphere system, which have been linked to oscillations in the strength of the vertical density gradient in the North Atlantic (Winton, 1993; Arzel et al., 2011; Peltier and Vettoretti, 2014), and to the existence of unstable states of the sea ice extent in the North Atlantic (Li, 2005; Li et al., 2010; Siddall et al., 2010; Petersen et al., 2013). In addition, there are features of the observational records that are inconsistent with iceberg armadas having been the driving force behind all episodes of abrupt climate change (Marshall and Koutnik, 2006). Periods of abrupt Greenland cooling are typically divided between 'Heinrich events', for which widespread ice-rafted detritus is found (Hemming, 2004), and 'Dansgaard-Oeschger stadials' (Dansgaard et al., 1993), which include all abrupt

Greenland coolings, but are not associated with widespread ice rafted detritus. In Greenland ice core records, Heinrich events are very similar to Dansgaard-Oeschger stadials, despite the apparent contrast in the associated amount of ice rafted detritus and, presumably, the consequent freshwater input.

What's more, the arrival of ice-rafted detritus does not seem to precede changes in the AMOC, where the two are recorded together. An analysis of Heinrich event 2 in the NW Atlantic showed that weakening of the AMOC preceded the widespread deposition of ice-rafted detritus by approximately 2 ky (Gutjahr and Lippold, 2011), while a statistical analysis of the temporal relationship between ice-rafted detritus near Iceland and dozens of cold events in Greenland suggested that ice-rafted detritus deposition generally lags the onset of cooling by a significant amount (Barker et al., 2015). These observations throw further doubt on the role of iceberg melting as the universal driver of abrupt climate change. In fact, it may be more likely that iceberg release is more often a consequence of AMOC interruptions, rather than necessarily being their cause, a possibility raised by the identifications of subsurface warming during AMOC interruptions in hosed model simulations (Mignot et al., 2007). Such intermediate-depth warming of the North Atlantic, resulting from the reduced release of oceanic heat at high latitudes, would have melted floating ice shelves at their bases, contributing to ice sheet collapse (Shaffer, 2004; Flückiger et al., 2006; Alvarez-Solas et al., 2010; Marcott et al., 2011). Thus, although there is good evidence that large iceberg armadas were released during most stadials, and would have freshened the North Atlantic accordingly, they were not necessarily the main causal factor involved in all stadials. This raises the question: does the global footprint of an AMOC interruption depend on its cause, or is any AMOC interruption the same, regardless of whether or not freshwater forcing was behind it? How does the importance of the causal driver compare with the sensitivity to the background climate state, itself determined by CO_2, terrestrial ice sheets, and the Earth's orbital parameters?

In order to explore these questions, we make use of a large number of long water-hosing simulations with CM2Mc, a state-of-the-art Earth System model, to show how the global response to hosing varies between a preindustrial and glacial background state, and under different orbital forcings. In addition, we take advantage of the fact that the same model exhibits previously undescribed spontaneous AMOC interruptions and resumptions, which appear very similar to stadial-interstadial variability, to reveal what aspects of the abrupt changes are a result of the hosing itself rather than consequences of the changing AMOC.

2 Experimental Setup

2.1 Model Description

The simulations shown here use the coupled ocean-atmosphere model CM2Mc, as described in Galbraith et al. (2011). This is a moderately low resolution, but full complexity model, that includes an atmospheric model that is at the high-complexity end of the spectrum applied in previously-published water hosing simulations. In brief, the model includes: a 3-degree finite volume atmospheric model, similar to the 2-degree version used in the GFDL CM2.1 (Anderson, 2004) and ESM2M (Dunne et al., 2012) models; MOM5, a non-Bousinnesq ocean model with a fully-nonlinear equation of state, subgridscale parameterizations for mesoscale and submesoscale turbulence, vertical mixing with the KPP scheme as well as due to the interaction of tidal waves with rough topography but otherwise a very low background vertical diffusivitity (0.1 cm^2 s^{-1}), similar to that used in the GFDL ESM2M model (Dunne et al., 2012); a sea-ice module, static land module, and a coupler to exchange fluxes between the components. In addition, the ocean model includes the BLING biogeochemical model as described in Galbraith et al. (2010). This includes limitation of phytoplankton growth by iron, light, temperature and phosphate, as well as a parameterization of ecosystem structure.

2.2 Experimental Design

The experiments shown here vary in terms of the prescribed atmospheric CO_2, the size of terrestrial ice sheets, and the Earth's orbital configuration (obliquity and precession). Terrestrial ice sheets were set to either the 'preindustrial' extents, or the full LGM reconstruction of the Paleoclimate Model Intercomparison Project 3 (https://pmip3.lsce.ipsl.fr), in which case the ocean bathymetry was also altered to represent lowered sea level, including a closed Bering Strait, and ocean salinity was increased by 1 PSU. Atmospheric CO_2 concentration has a value of either 270 or 180 ppm depending on whether the ice sheets have a preindustrial or glacial extent, respectively. The obliquity was set to either 22.0°or 24.5°, spanning the calculated range of the last 5 My (Laskar et al., 2004). The precessional phase, defined as the angle between the Earth's position during the northern hemisphere autumnal equinox and the perihelion, was set to two opposite positions, corresponding to the positions at which the boreal seasonalities are least and most severe (90°and 270°, respectively). All other boundary conditions of the model were configured as described in Galbraith et al. (2011).

Freshwater forcing ('hosing') was applied to four simulations run under 'Preindustrial' conditions with the four possible combinations of obliquity and precession, and a corresponding four under 'Glacial' conditions. For each of these eight hosing simulations, the model was initialized from a previous preindustrial or LGM state, run for 1000 years, a freshwater hosing was applied for 1000 years, and then it was run for a further 1000 years with the hosing off. Control simulations (without hosing) were also run for the same length of time as the hosing to allow drift correction. During hosing, freshwater was added in the North Atlantic by overriding the land-to-ocean ice calving flux with a preindustrial annual mean plus an additional 0.2 Sv evenly distributed in a rectangle bounded by 40N to 60N and 60W to 12W. Because the same preindustrial mean background calving flux was used in all hosings, for the five non-preindustrial hosings, this also represents a 0.018 Sv increase in the calving flux on the Antarctic coast relative to the background glacial climate. It should be noted that because the model does not have a rigid lid, this represents a ‘real’ freshwater input to the ocean. The result is a global sea level rise of 17 m over the 1000 year hosing, representing approximately one third the maximum rate of sea level rise estimated during the last deglaciation (Melt Water Pulse 1a) (Deschamps et al., 2012). For the top panels of Figures 5-10, the ‘weak’ AMOC state is defined as years 901-1000 of hosing, and the ’strong’ AMOC state is the same century taken from the corresponding control simulation to correct for drift, which was quite small.

In addition, we show results from a simulation for which hosing was not applied, but which exhibits spontaneous oscillations in the AMOC reminiscent of D-O events. This ‘Unhosed’ simulation was conducted under glacial CO_2 (180 ppm), but with preindustrial ice sheets and bathymetry, low obliquity, and weak boreal seasonality. The Unhosed simulation was one of a suite of simulations integrated with constant forcing, under the same simultaneous changes in obliquity, precession and ice sheet configuration described above but under a broader range of CO_2 variations (Galbraith et al., in prep). The strength of the AMOC varies considerably among these simulations, with stronger AMOC occurring at high CO_2 and with full glacial ice sheets (Figure 1), for reasons that will be discussed elsewhere (Galbraith et al., in prep). Strikingly, two of the simulations (those with 180 ppm CO_2, low obliquity, and preindustrial ice sheets) were found to show oscillations between two unstable states of the AMOC, reminiscent of D-O changes (Figure 1). Of these, the simulation with weak boreal seasonality gradually settled into longer oscillations with a period of ~1200 yrs, closer to the period of the observed D-O cycles, after a few millennia of more rapid oscillations. Given the greater similarity to the period of observed D-O cycles, this simulation is taken as the ’Unhosed’ example. In this Unhosed simulation, the weak AMOC state is defined by averaging the last century of an ’unforced’ AMOC decrease (model years 7501-7600) and the strong AMOC state is defined by averaging a century following an ’unforced’ AMOC increase (model years 7901-8000).

The final experiment is a modification of the Unhosed simulation, in which the 0.2 Sv hosing perturbation is applied to the North Atlantic during a strong-AMOC interval. This final experiment provides an explicit test of the effect of a hosed vs. an unhosed AMOC weakening.

3 Results

3.1 Simulated changes in the North Atlantic

The eight hosed simulations show a number of common features in the North Atlantic, which vary as a function of boundary conditions (Figure 2). Within the first two centuries of hosing, the Greenland temperature rapidly drops by 8-15 °C, with a stronger response under high obliquity. When the hosing is stopped, the temperatures abruptly increase by 8-20 °C, again with a stronger response under high obliquity, and under glacial conditions. Overall, the simulated magnitudes of warming and cooling are of the same magnitude as reconstructed for abrupt climate change from Greenland ice cores (Buizert et al., 2014). The AMOC follows a very similar temporal progression in all cases, which is the inverse of the sea ice extent in the North Atlantic. The average North Atlantic sea surface salinity drops by 2-4 PSU in the hosed simulations, consistent with the generally-accepted mechanism of a halocline strengthening due to freshwater forcing, associated with an expansion of sea ice, being the cause of an AMOC interruption. Thus, as shown by many prior simulations, the hosing response is quite consistent with observations and the idea of iceberg armadas shutting down the AMOC and initiating abrupt climate change (Kageyama et al., 2013; Menviel et al., 2014).

However, Figure 2 also shows the same metrics of North Atlantic variability for the Unhosed simulation. Under the low CO_2, low obliquity and preindustrial ice-sheets of this simulation, the model's coupled ocean-atmosphere system causes the AMOC to spontaneously oscillate between 15-18 Sv and 6 Sv, on a centennial timescale (Figures 2, 3). Although the amplitude of the variations in the Unhosed simulation tends to be smaller than in the hosed simulations, with a weaker AMOC throughout (Figure 3), the general relationship between the four variables is quite similar (Figure 2). When AMOC is weak, North Atlantic deep convection is greatly reduced and shifted to the south, while sea ice expands in the northeast Atlantic, in both the hosed and Unhosed simulations (Figure 4). Thus, the Unhosed oscillations are also consistent with observational evidence that a strengthened halocline, associated with an expansion of sea ice, were coupled to a weakening of the AMOC - even in the absence of external freshwater forcing. This variability follows in the long tradition of spontaneous AMOC oscillations observed among simpler models, and appears to be very similar to the unforced AMOC oscillation observed recently in the Community Earth System (CESM) model, which is of similar complexity but run at higher resolution, by Peltier and Vettoretti (2014).

The spontaneous millennial AMOC oscillations that occur in ocean circulation models can generally be described as 'deep decoupling oscillations' (Winton, 1993). These oscillations include a weak overturning phase, during which convection is reduced and/or shifted to lower latitudes (Goosse, 2002), allowing the deep polar ocean to accumulate heat, transported northwards by diffusion at depth. The accumulation of heat gradually destabilizes the polar water column, until deep convection resumes in a 'thermohaline flush' (Weaver and Sarachik, 1991). The reinvigorated overturning carries salty subtropical waters north, further strengthening the overturning (Stommel, 1961; Rooth, 1982). A gradual decrease of the poleward surface temperature gradient (Arzel et al., 2010) and/or salinity gradient (Peltier and Vettoretti, 2014) causes a gradual weakening of the overturning, until some point at which the AMOC weakens nonlinearly and the weak phase returns. It has been suggested that expansions of sea ice, which tend to amplify the polar halocline by exporting brines to depth and building up fresh layers due to melt at the surface, could have been key to stratifying the northern North Atlantic and driving the AMOC into its weak mode (Kaspi et al., 2004; Li, 2005; Dokken et al., 2013).

The changes in AMOC, sea ice and surface salinity in the Unhosed simulation (Figure 2) are consistent with this general scenario. It is remarkable that the magnitude of the salinity change in the unforced simulations is on the order of more than 1 PSU, nearly half as much as for the hosing simulation under the same CO_2 and orbital configuration (Figure 2), in spite of the absence of any external sources of freshwater, and a reduction of precipitation relative to evaporation over the North Atlantic. The surface freshening is therefore caused by the changes in ocean circulation and sea ice cycling. Figure 5 shows that, during the weak AMOC phase, heat accumulates at depth in the North Atlantic due to the northward diffusion of warm waters from the tropics and lack of flushing by cold North Atlantic Deep Water (Palter et al., 2014). At the same time, the salinity increases at the tropical Atlantic surface (Peltier and Vettoretti, 2014), and the poleward surface temperature gradient intensifies (Arzel et al., 2010). Paleoceanographic reconstructions from D-O events are consistent with both the accumulation of tropical sea surface salinity (Schmidt et al., 2006) and the simulated changes in water column temperature and salinity in the Nordic seas (Dokken et al., 2013). The buildup of heat at intermediate depths in the subpolar North Atlantic helps to weaken the stratification (Supplementary Figure 7), so that it can be overcome when a saline surface anomaly disrupts the halocline, triggering deep convection. Given that changes in temperature have a significant role, in addition to changes in salinity, it would appear most appropriate to call the mechanism in the Unhosed simulation a 'thermohaline oscillator', rather than the simpler 'salt oscillator' described by (Peltier and Vettoretti, 2014).

Next, we show how the global consequences of changes in the AMOC depend on the background climate state, and the question of whether or not they are forced by freshwater addition. We do so by exploring a few key atmospheric and oceanic variables that have well-documented responses to abrupt climate change as recorded by paleoclimate records.

3.2 Global atmospheric response

Abrupt climate change was initially identified in ice core proxy records of atmospheric temperature, and subsequently extended to temperature variations recorded in multiple proxies from around the world (Clement and Peterson, 2008). Figure 6 summarizes the global surface air temperature change that occurs in response to our simulated AMOC interruptions. The first order patterns of surface air temperature change are very similar between the preindustrial and glacial boundary conditions, as well as in the unhosed simulation. The northern hemisphere undergoes general cooling in the extratropics, with greatest cooling in the North Atlantic from Iceland to Iberia, and with cooling extending into the tropics of the North Atlantic, North Africa, and southeast Asia. Meanwhile, the southern hemisphere warms everywhere except in the western tropical Pacific and Indian oceans. The maximum warming occurs at high latitudes of the Southern Ocean, and is associated with a sea ice retreat (Figure 5). The general temperature pattern is consistent with the idea of a bipolar seesaw (Broecker, 1998; Stocker and Johnsen, 2003).

One notable difference in the spatial patterns is the temperature change in the N Pacific, including the western margin of Canada and southern Alaska. The temperature here is quite sensitive to the degree of northward transport of warm ocean water from the subtropical gyre, which is quite variable between simulations. All hosed simulations develop a Pacific Meridional Overturning Circulation (PMOC) when the AMOC weakens, previously described in models as an Atlantic-Pacific Seesaw (Saenko et al., 2004; Okumura et al., 2009; Okazaki et al., 2010; Chikamoto et al., 2012; Hu et al., 2012). The degree to which a PMOC develops varies substantially between simulations, with stronger development of PMOC in the preindustrial hosings. The development of a strong PMOC counteracts the hemisphere-wide cooling in the NE Pacific, which can actually cause a warming. This suggests that temperature proxy records from this region would provide strong observational constraints on the degree to which a PMOC developed during abrupt climate changes. The simulations that develop a strong PMOC also show a region of maximum cooling at the Kuroshio-Oyashio confluence, consistent with a southward shift in the front.

The strength of the bipolar seesaw also varies significantly as a function of background climate state, due to differences in both the southern hemisphere and the North Atlantic. Stronger southern warming occurs under glacial conditions, and with the combination of high obliquity and strong boreal seasons (Supplementary Figure 2). The temperature response to hosing in the North Atlantic is particularly dependant on orbital configurations in glacial simulations because of different initial sea-ice extents which are strongly driven by obliquity (Figure 2, 3rd row, compare initial sea ice area under glacial and preindustrial).

In general, the temperature response in the Unhosed simulation is very similar to the ensemble means of the hosed simulations, and would appear to have a relatively weak southern warming. The weak southern warming is partly due to the fact that southern warmings develop slowly, and the time between the Unhosed ’stadial’ and ’interstadial’ is relatively short (~400 yrs). If the ’interstadial’ reference years are taken at the end of an interstadial, rather then the middle, a stronger southern warming, more similar to that of preindustrial hosed simulations, is observed (Supplementary Figure 8). The spatial differences between the Unhosed and the hosed simulations are generally of the same order as the differences among the hosed simulations under different background states.

Changes in precipitation during abrupt climate changes have also been well-documented in speleothems and marine sediment records (Peterson, 2000; Wang et al., 2001; Carolin et al., 2013). As shown in Figure 7, the overall patterns of change are similar between hosed and Unhosed simulations, as they were for the changes in temperature. The robust, common patterns include reduced precipitation over the North Atlantic, a southward shift of the Intertropical Convergence Zone (ITCZ), previously shown to be a direct result of the sea ice expansion associated with stadials (Chiang and Bitz, 2005), and reduced precipitation over south Asia.

In fact, many aspects of the precipitation changes vary more as a function of background climate state, including orbital configuration, than they do between hosed and Unhosed (Supplementary Figure 3). Thus, not only is the mean state of tropical precipitation sensitive to orbital forcing (Clement et al., 2004), but the response of tropical precipitation to an AMOC disruption is sensitive to orbital forcing as well. Perhaps the two most notable differences among the simulations are the pattern of change surrounding the west Pacific warm pool, an extremely dynamic region with heavy precipitation, and the NE Pacific and western North America, where changes in precipitation follow the sea surface temperature through its control on water moisture content and atmospheric circulation. The response to hosing in the region surrounding the west Pacific warm pool, including Indonesia and NE Australia, is strongly dependant on precession (Supplementary Figure 3). For example, with weak boreal seasons, hosing tends to cause an increase in precipitation north of Borneo, which does not occur when boreal seasons are strong.

3.3 Global ocean biogeochemistry response

The observed footprint of abrupt climate change also extends to ocean biogeochemistry, with pronounced and well-documented changes in both dissolved oxygen concentrations and export production. Prior work has shown that many aspects of the observed oxygenation changes (Schmittner et al., 2007b) and export production changes (Schmittner, 2005; Mariotti et al., 2012) can be well reproduced by coupled ocean-biogeochemistry models under hosing experiments.

As shown by Figure 8, our model simulations produce consistent changes in intermediate-depth oxygen during AMOC weakening, hosed or unhosed, that agree well with the bipolar seesaw-mode changes in oxygenation extracted from sediment proxy records of the last deglaciation (Galbraith and Jaccard, 2015). All simulations show a decrease of oxygen throughout the full depth of the North Atlantic, due to the lack of ventilated North Atlantic Deep Water, and an increase in the oxygenation of the intermediate-depth North Pacific and Arabian Sea. We note that the North Pacific changes reveal a pronounced shift in the southeastward penetration of North Pacific Intermediate Water, with a hotspot of oxygen change where the edge of the strongly-ventilated thermocline impinges on the California margin. This hotspot implies that a tendency for a frontal shift to occur in this region makes it particularly sensitive to changes in the AMOC, and explains why the California borderlands region has such rich records of oxygenation changes on millennial timescales (Behl and Kennett, 1996; Hendy and Kennett, 1999; Cartapanis et al., 2011).

The relative changes in export production, shown in Figure 9, are locally quite large (in excess of 100%) but have weaker regional patterns that are less consistent between simulations. The most consistent strong features are a reduction of export in the northern North Atlantic, the western tropical North Atlantic, and the southern margin of the Indo-Pacific subtropical gyre, and an increase in export off of NW Africa, to the west of California, and in the high latitude Southern Ocean. Regions that do not always respond consistently are the subarctic Pacific, which depends significantly on whether or not a PMOC develops, and the Pakistani margin, which shows an increase in export under pre-industrial, but not glacial hosing. It is important to point out that, because the model does not resolve coastal upwellings, it is probably missing important changes. This may explain, for example, the fact that decreases in primary production are not simulated on the Baja California margin during hosings, as reconstructed during stadials (Cartapanis et al., 2011). In general, the differences between the various hosed simulations is as large as the difference between hosed and unhosed.

The simulated changes of export production show an overall decrease globally, consistent with prior results (Schmittner, 2005; Schmittner et al., 2007b; Mariotti et al., 2012), which contributes to the simulated increase of intermediate-depth oxygen concentrations during stadials by reducing oxygen consumption. In addition, oxygen supply to intermediate depths of the northern Indo-Pacific is increased by more rapid flushing of thermocline waters during stadials, indicated by lower ventilation ages (Figure 10), also consistent with other models (Schmittner et al., 2007b). The primary discrepancies in intermediate-depth age between the simulations are in the subarctic Pacific, again related to the development of a PMOC, changes in ventilation in the Tropical Atlantic thermocline, and in the degree of ventilation changes in the Southern Ocean.

3.4 Hosing the Unhosed

The analyses above suggest that most of the large-scale responses of climate and ocean biogeochemistry to an AMOC disruption are similar regardless of whether the interruption is forced through hosing or as a spontaneous result of internal model dynamics. In order to further test this apparent insensitivity to the cause of AMOC weakening, we applied a freshwater forcing during a strong AMOC interval of the Unhosed simulation, forcing the model to return to a weak AMOC state earlier than in the standard Unhosed case. This experiment provides a direct comparison between an unforced and a freshwater forced AMOC reduction. The freshwater forcing weakens the AMOC transport (Figure 2, black line in 3rd column), and maintains its weakened state over the full 1000 year simulation, whereas the Unhosed simulation returns to the strong-AMOC state after about 800 years. By comparing both the forced and unforced simulations after 800 years of stadial, we can estimate the differences caused by the freshwater itself.

The changes caused by the freshwater addition are shown in Figure 11, which can be compared with the Unhosed variability in Figures 6, 7, 8, and 9. The change in surface air temperatures differs little as a result of the hosing, with significant contrasts only in the North Atlantic, North Pacific, and high latitude Southern Ocean. Precipitation shows a much larger response under hosing, which is generally an amplification of the Unhosed trends, though the impact over western Indonesia is a uniformly strong drying rather than the mixed response of the Unhosed case. Dissolved oxygen also shows an amplification of the Unhosed trends when hosed, though the changes are relatively small, while export production shows changes mainly in the N Atlantic and NE Pacific. The general amplification of changes can be understood by the fact that the freshwater-forced simulation has a weaker AMOC, and more extensive North Atlantic sea-ice coverage, leading to lower temperatures in the NE Atlantic and a correspondingly greater response in atmospheric circulation that amplifies most features of the weak-AMOC state.

The fact that precipitation responds most strongly suggests that, among the metrics examined here, it has the greatest sensitivity to the intensification of the Unhosed stadial by hosing, which could reflect a fairly direct link between the northern sea ice edge and/or North Atlantic cooling, latitudinal sea surface temperature gradients, and the Hadley circulation (Chiang and Bitz, 2005; Chiang and Friedman, 2012). Essentially, a stronger push from the northern extratropics leads to a stronger response in the tropical hydrological cycle. Observations showing that precipitation responses were markedly different during Heinrich stadials as opposed to non-Heinrich stadials in Borneo (Carolin et al., 2013), northeastern Brazil (Wang et al., 2004) and the Cariaco basin (Deplazes et al., 2013) are therefore consistent with Heinrich stadials representing much stronger interruptions of the AMOC (Böhm et al., 2015), that led to greater sea ice expansion and North Atlantic cooling, and consequently larger shifts in tropical precipitation.

Apart from the amplification of the general trends, we note one distinct additional feature: the southern hemisphere warming is decreased under hosing, weakening the bipolar seesaw. This feature of the Antarctic response appears to reflect the transport of freshwater from the North Atlantic to the Southern Ocean, in addition to the small increase in calving flux from the Antarctic margin (Supplementary Figure 9), so that the Southern Ocean surface is freshened. The addition of freshwater strengthens the Southern Ocean halocline, reducing ocean heat release and keeping a larger mantle of sea ice around Antarctica. Thus, the cooler Southern Ocean does not reflect a different response to the AMOC weakening itself, but rather a secondary effect of the freshwater addition through its direct influence on the vertical density structure of the Southern Ocean. We note that Schmittner et al. (2007a) found an opposite effect of freshwater input on the Southern Ocean, with a relative weakening of the halocline causing a destratification of the Southern Ocean under freshwater forcing. It would thus appear that this aspect of hosing is quite sensitive to model behaviour and experimental design. Given the potential importance of Southern Ocean convection on modifying atmospheric CO_2 (Sarmiento and Toggweiler, 1984; Sigman et al., 2010; Bernardello et al., 2014; Jaccard et al., 2016), careful consideration should be made of freshwater input to the Southern Ocean derived from the melting of local Antarctic (Weaver et al., 2003; Golledge et al., 2014) or distant northern hemisphere ice sheets.

4 Discussion and conclusions

Our Unhosed model simulation adds to a small, but growing subset of complex 3-dimensional ocean-atmosphere model simulations exhibiting unforced oscillations similar to the abrupt climate changes of Dansgaard-Oeschger cycles. Under a particular set of boundary conditions (low CO_2, with preindustrial ice sheets and low obliquity), it spontaneously oscillates between strong and weak AMOC states, triggered by internal climate variability within the model, acting on a type of 'thermohaline oscillator'.

The Unhosed simulation was integrated under perfectly stable boundary conditions, with no variability in external factors such as solar output, aerosols or freshwater runoff. Such additional variability might make it easier for spontaneous AMOC variations to occur in reality, as long as the AMOC is in relatively a weak state due to the background climate state, leading to AMOC oscillations under a wider range of background conditions. Thus, large volcanic eruptions (Pausata et al., 2015), ice-sheet topography changes (Zhang et al., 2014) or solar variability could all potentially trigger an abrupt change in the real world, without requiring freshwater input, even when the climate system is in a more stable mode than that of the Unhosed simulation. Nonetheless, the fact that weakening of the AMOC always occurs in models under sufficient hosing implies that, even in a strong mode, the AMOC is vulnerable to freshwater forcing, if it is large enough.

As previously suggested, melting of floating ice shelves due to subsurface ocean warming could provide an important feedback to an initial AMOC weakening, accelerating ice sheet mass loss due to their buttressing-effect on upstream ice, and adding freshwater that would push the AMOC into a very weak mode (Marshall and Koutnik, 2006; Alvarez-Solas et al., 2010; Marcott et al., 2011). Such a behaviour is similar to that exhibited here by the Hosed-Unhosed simulation, and may have been necessary to produce a complete ‘shutdown’ of the AMOC, as suggested by Pa/Th measurements at Bermuda Rise (Böhm et al., 2015). This suggests that the question of whether or not a Heinrich event occurred during an AMOC interruption had more to do with the susceptibility of the Laurentide ice sheet to collapse than the nature of the initial AMOC interruption itself. In turn, the degree to which consequent ice sheet melting altered ocean circulation may have depended on where the freshwater was discharged, including how much of the freshwater was input to the ocean as sediment-laden hyperpycnal flows (Tarasov and Peltier, 2005; Roche et al., 2007).

Although they only occur in our model under an unrealistic combination of boundary conditions, the spontaneous nature of these oscillations allows a powerful comparison to be made with the more typical freshwater-hosed simulations of AMOC weakening. When compared with the Hosed simulations, the general features of the atmospheric and oceanic responses are remarkably robust, with climate background state playing as great a role in determining the response as whether the AMOC weakening was spontaneous or forced. These robust features can therefore be taken to reflect consistent dynamical changes related to the AMOC interruption and its coupling with sea ice and atmospheric changes, independent of the ultimate cause of the AMOC interruption. Of the variables examined here, tropical precipitation showed the strongest sensitivity to an intensification of AMOC interruption with additional hosing.

An important difference between Hosed and Unhosed simulations lay in the direct impact of freshwater on ocean density structure. Polar haloclines are very sensitive to freshwater input, which can stratify or destratify them depending on the depth at which freshwater is injected. In our simulations, an important consequence of this is the stratification of the Southern Ocean, which could have important consequences for atmospheric CO_2. Aside from this contrast, the global features of an

AMOC weakening appear to depend just as much on the background climate state as they do on its fundamental cause.

Acknowledgements. We thank the Canadian Foundation for Innovation (CFI) and an allocation to the Scinet supercomputing facility (University of Toronto), made through Compute Canada, for providing the computational resources. We are grateful to Olivier Arzel, two anonymous reviewers, and editor Gerrit Lohmann for constructive comments that greatly improved the manuscript.

References

Alley, R. B., Marotzke, J., Nordhaus, W. D., Overpeck, J. T., Peteet, D. M., Pielke, R. A., Pierrehumbert, R. T., Rhines, P. B., Stocker, T. F., Talley, L. D., and Wallace, J. M.: Abrupt climate change., Science (New York, N.Y.), 299, 2005–10, doi:10.1126/science.1081056, http://www.sciencemag.org/content/299/5615/2005.abstract, 2003.

Alvarez-Solas, J., Charbit, S., Ritz, C., Paillard, D., Ramstein, G., and Dumas, C.: Links between ocean temperature and iceberg discharge during Heinrich events, Nature Geoscience, 3, 122–126, doi:10.1038/ngeo752, http://dx.doi.org/10.1038/ngeo752, 2010.

Anderson, J. L.: The New GFDL Global Atmosphere and Land Model AM2–LM2: Evaluation with Prescribed SST Simulations, Journal of Climate, 17, 4641–4673, doi:10.1175/JCLI-3223.1, http://journals.ametsoc.org/doi/abs/10.1175/JCLI-3223.1, 2004.

Arzel, O., Colin de Verdière, A., and England, M. H.: The Role of Oceanic Heat Transport and Wind Stress Forcing in Abrupt Millennial-Scale Climate Transitions, Journal of Climate, 23, 2233–2256, doi:10.1175/2009JCLI3227.1, http://journals.ametsoc.org/doi/abs/10.1175/2009JCLI3227.1, 2010.

Arzel, O., England, M. H., Verdière, A. C., and Huck, T.: Abrupt millennial variability and interdecadal-interstadial oscillations in a global coupled model: sensitivity to the background climate state, Climate Dynamics, 39, 259–275, doi:10.1007/s00382-011-1117-y, http://dx.doi.org/10.1007/s00382-011-1117-y, 2011.

Barker, S., Chen, J., Gong, X., Jonkers, L., Knorr, G., and Thornalley, D.: Icebergs not the trigger for North Atlantic cold events, Nature, 520, 333–336, doi:10.1038/nature14330, http://dx.doi.org/10.1038/nature14330, 2015.

Behl, R. J. and Kennett, J. P.: Brief interstadial events in the Santa Barbara basin, NE Pacific, during the past 60 kyr, Nature, 379, 243–246, doi:10.1038/379243a0, http://dx.doi.org/10.1038/379243a0, 1996.

Bernardello, R., Marinov, I., Palter, J. B., Galbraith, E. D., and Sarmiento, J. L.: Impact of Weddell Sea deep convection on natural and anthropogenic carbon in a climate model, Geophysical Research Letters, 41, 7262–7269, doi:10.1002/2014GL061313, http://doi.wiley.com/10.1002/2014GL061313, 2014.

Böhm, E., Lippold, J., Gutjahr, M., Frank, M., Blaser, P., Antz, B., Fohlmeister, J., Frank, N., Andersen, M. B., and Deininger, M.: Strong and deep Atlantic meridional overturning circulation during the last glacial cycle, Nature, 517, 73–76, doi:10.1038/nature14059, http://dx.doi.org/10.1038/nature14059, 2015.

Broecker, W. S.: Massive iceberg discharges as triggers for global climate change, 1994.

Broecker, W. S.: Paleocean circulation during the Last Deglaciation: A bipolar seesaw?, Paleoceanography, 13, 119–121, doi:10.1029/97PA03707, http://doi.wiley.com/10.1029/97PA03707, 1998.

Buizert, C., Gkinis, V., Severinghaus, J. P., He, F., Lecavalier, B. S., Kindler, P., Leuenberger, M., Carlson, A. E., Vinther, B., Masson-Delmotte, V., White, J. W. C., Liu, Z., Otto-Bliesner, B., and Brook, E. J.: Greenland temperature response to climate forcing during the last deglaciation., Science (New York, N.Y.), 345, 1177–80, doi:10.1126/science.1254961, http://www.sciencemag.org/content/345/6201/1177.short, 2014.

Carolin, S. A., Cobb, K. M., Adkins, J. F., Clark, B., Conroy, J. L., Lejau, S., Malang, J., and Tuen, A. A.: Varied response of western Pacific hydrology to climate forcings over the last glacial period., Science (New York, N.Y.), 340, 1564–6, doi:10.1126/science.1233797, http://science.sciencemag.org/content/340/6140/1564.abstract, 2013.

Cartapanis, O., Tachikawa, K., and Bard, E.: Northeastern Pacific oxygen minimum zone variability over the past 70 kyr: Impact of biological production and oceanic ventilation, Paleoceanography, 26, n/a–n/a, doi:10.1029/2011PA002126, http://doi.wiley.com/10.1029/2011PA002126, 2011.

Chiang, J. C. and Friedman, A. R.: Extratropical Cooling, Interhemispheric Thermal Gradients, and Tropical Climate Change, Annual Review of Earth and Planetary Sciences, 40, 383–412, doi:10.1146/annurev-earth-042711-105545, http://www.annualreviews.org/doi/abs/10.1146/annurev-earth-042711-105545, 2012.

Chiang, J. C. H. and Bitz, C. M.: Influence of high latitude ice cover on the marine Intertropical Convergence Zone, Climate Dynamics, 25, 477–496, doi:10.1007/s00382-005-0040-5, http://link.springer.com/10.1007/s00382-005-0040-5, 2005.

Chikamoto, M. O., Menviel, L., Abe-Ouchi, A., Ohgaito, R., Timmermann, A., Okazaki, Y., Harada, N., Oka, A., and Mouchet, A.: Variability in North Pacific intermediate and deep water ventilation during Heinrich events in two coupled climate models, Deep Sea Research Part II: Topical Studies in Oceanography, 61-64, 114–126, doi:10.1016/j.dsr2.2011.12.002, http://www.sciencedirect.com/science/article/pii/S0967064511002517, 2012.

Clark, P. U., Pisias, N. G., Stocker, T. F., and Weaver, A. J.: The role of the thermohaline circulation in abrupt climate change., Nature, 415, 863–9, doi:10.1038/415863a, http://dx.doi.org/10.1038/415863a, 2002.

Clement, A. C. and Peterson, L. C.: Mechanisms of abrupt climate change of the last glacial period, Reviews of Geophysics, 46, RG4002, doi:10.1029/2006RG000204, http://doi.wiley.com/10.1029/2006RG000204, 2008.

Clement, A. C., Hall, A., and Broccoli, A. J.: The importance of precessional signals in the tropical climate, Climate Dynamics, 22, 327–341, doi:10.1007/s00382-003-0375-8, http://link.springer.com/10.1007/s00382-003-0375-8, 2004.

Colin de Verdière, A.: A Simple Model of Millennial Oscillations of the Thermohaline Circulation, Journal of Physical Oceanography, 37, 1142–1155, doi:10.1175/JPO3056.1, http://journals.ametsoc.org/doi/abs/10.1175/JPO3056.1, 2007.

Dansgaard, W., Johnsen, S. J., Clausen, H. B., Dahl-Jensen, D., Gundestrup, N., Hammer, C. U., and Oeschger, H.: North Atlantic climatic oscillations revealed by deep Greenland ice cores, Geophysical Monograph Series, Climate Processes and Climate Sensitivity, 29, 288–298, doi:10.1029/GM029p0288, http://onlinelibrary.wiley.com/doi/10.1029/GM029p0288/summary, 1984.

Dansgaard, W., Johnsen, S. J., Clausen, H. B., Dahl-Jensen, D., Gundestrup, N. S., Hammer, C. U., Hvidberg, C. S., Steffensen, J. P., Sveinbjornsdottir, A. E., Jouzel, J., and Bond, G.: Evidence for general instability of past climate from a 250-kyr ice-core record, Nature, 364, 218–220, http://dx.doi.org/10.1038/364218a0, 1993.

Deplazes, G., Lückge, A., Peterson, L. C., Timmermann, A., Hamann, Y., Hughen, K. A., Röhl, U., Laj, C., Cane, M. A., Sigman, D. M., and Haug, G. H.: Links between tropical rainfall and North Atlantic climate during the last glacial period, Nature Geoscience, 6, 213–217, doi:10.1038/ngeo1712, http://dx.doi.org/10.1038/ngeo1712, 2013.

Deschamps, P., Durand, N., Bard, E., Hamelin, B., Camoin, G., Thomas, A. L., Henderson, G. M., Okuno, J., and Yokoyama, Y.: Ice-sheet collapse and sea-level rise at the Bolling warming 14,600 years ago., Nature, 483, 559–64, doi:10.1038/nature10902, http://dx.doi.org/10.1038/nature10902, 2012.

Dokken, T. M., Nisancioglu, K. H., Li, C., Battisti, D. S., and Kissel, C.: Dansgaard-Oeschger cycles: Interactions between ocean and sea ice intrinsic to the Nordic seas, Paleoceanography, 28, 491–502, doi:10.1002/palo.20042, http://doi.wiley.com/10.1002/palo.20042, 2013.

Drijfhout, S., Gleeson, E., Dijkstra, H. A., and Livina, V.: Spontaneous abrupt climate change due to an atmospheric blocking-sea-ice-ocean feedback in an unforced climate model simulation., Proceedings of the National Academy of Sciences of the United States of America, 110, 19 713–8, doi:10.1073/pnas.1304912110, http://www.pnas.org/content/110/49/19713.short, 2013.

Dunne, J. P., John, J. G., Adcroft, A. J., Griffies, S. M., Hallberg, R. W., Shevliakova, E., Stouffer, R. J., Cooke, W., Dunne, K. A., Harrison, M. J., Krasting, J. P., Malyshev, S. L., Milly, P. C. D., Phillipps, P. J., Sentman, L. T., Samuels, B. L., Spelman, M. J., Winton, M., Wittenberg, A. T., and Zadeh, N.: GFDL's ESM2 Global Coupled Climate-Carbon Earth System Models. Part I: Physical Formulation and Baseline Simulation Characteristics., Journal of Climate, 25, 6646–6665, 10.1175/JCLI-D-11-00560.1http://search.ebscohost.com/login.aspx?direct=true{&}db=a9h{&}AN=82213818, 2012.

Fanning, A. F. and Weaver, A. J.: Temporal-geographical meltwater influences on the North Atlantic conveyor: Implications for the Younger Dryas, Paleoceanography, 12, 307–320, doi:10.1029/96PA03726, http://doi.wiley.com/10.1029/96PA03726, 1997.

Flückiger, J., Knutti, R., and White, J. W. C.: Oceanic processes as potential trigger and amplifying mechanisms for Heinrich events, Paleoceanography, 21, PA2014, doi:10.1029/2005PA001204, http://doi.wiley.com/10.1029/2005PA001204, 2006.

Friedrich, T., Timmermann, A., Menviel, L., Elison Timm, O., Mouchet, A., and Roche, D. M.: The mechanism behind internally generated centennial-to-millennial scale climate variability in an earth system model of intermediate complexity, Geoscientific Model Development, 3, 377–389, doi:10.5194/gmd-3-377-2010, http://www.geosci-model-dev.net/3/377/2010/gmd-3-377-2010.html, 2010.

Galbraith, E. D. and Jaccard, S. L.: Deglacial weakening of the oceanic soft tissue pump: global constraints from sedimentary nitrogen isotopes and oxygenation proxies, Quaternary Science Reviews, 109, 38–48, doi:10.1016/j.quascirev.2014.11.012, http://www.sciencedirect.com/science/article/pii/S0277379114004697, 2015.

Galbraith, E. D., Gnanadesikan, A., Dunne, J. P., and Hiscock, M. R.: Regional impacts of iron-light colimitation in a global biogeochemical model, Biogeosciences, 7, 1043–1064, doi:10.5194/bg-7-1043-2010, http://www.biogeosciences.net/7/1043/2010/bg-7-1043-2010.html, 2010.

Galbraith, E. D., Kwon, E. U. N. Y., Gnanadesikan, A., Rodgers, K. B., Griffies, S. M., Bianchi, D., Sarmiento, J. L., Dunne, J. P., Simeon, J., Slater, R. D., Wittenberg, A. T., and Held, I. M.: Climate Variability and Radiocarbon in the CM2Mc Earth System Model., Journal of Climate, 24, 4230–4254, 10.1175/2011JCLI3919.1http://search.ebscohost.com/login.aspx?direct=true{&}db=a9h{&}AN=65153947, 2011.

Ganopolski, A. and Rahmstorf, S.: Rapid changes of glacial climate simulated in a coupled climate model, Nature, 409, 153–158, 2001.

Ganopolski, A. and Rahmstorf, S.: Abrupt glacial climate changes due to stochastic resonance., Physical review letters, 88, 038 501, doi:10.1103/PhysRevLett.88.038501, 2002.

Golledge, N. R., Menviel, L., Carter, L., Fogwill, C. J., England, M. H., Cortese, G., and Levy, R. H.: Antarctic contribution to meltwater pulse 1A from reduced Southern Ocean overturning., Nature communications, 5, 5107, doi:10.1038/ncomms6107, http://www.nature.com/ncomms/2014/140929/ncomms6107/full/ncomms6107.html?WT.ec{_}id=NCOMMS-20141001, 2014.

Gong, X., Knorr, G., Lohmann, G., and Zhang, X.: Dependence of abrupt Atlantic meridional ocean circulation changes on climate background states, Geophysical Research Letters, 40, 3698–3704, doi:10.1002/grl.50701, http://doi.wiley.com/10.1002/grl.50701, 2013.

Goosse, H.: Potential causes of abrupt climate events: A numerical study with a three-dimensional climate model, Geophysical Research Letters, 29, 1860, doi:10.1029/2002GL014993, http://doi.wiley.com/10.1029/2002GL014993, 2002.

Gutjahr, M. and Lippold, J.: Early arrival of Southern Source Water in the deep North Atlantic prior to Heinrich event 2, Paleoceanography, 26, n/a–n/a, doi:10.1029/2011PA002114, http://doi.wiley.com/10.1029/2011PA002114, 2011.

Hall, a. and Stouffer, R. J.: An abrupt climate event in a coupled ocean-atmosphere simulation without external forcing., Nature, 409, 171–174, doi:10.1038/35051544, 2001.

Harrison, S. and Sanchez Goñi, M.: Global patterns of vegetation response to millennial-scale variability and rapid climate change during the last glacial period, Quaternary Science Reviews, 29, 2957–2980, doi:10.1016/j.quascirev.2010.07.016, http://www.sciencedirect.com/science/article/pii/S0277379110002787, 2010.

Heinrich, H.: Origin and consequences of cyclic ice rafting in the Northeast Atlantic Ocean during the past 130,000 years, Quaternary Research, 29, 142–152, doi:10.1016/0033-5894(88)90057-9, http://www.sciencedirect.com/science/article/pii/0033589488900579, 1988.

Hemming, S. R.: Heinrich events: Massive late Pleistocene detritus layers of the North Atlantic and their global climate imprint, Reviews of Geophysics, 42, RG1005, doi:10.1029/2003RG000128, http://doi.wiley.com/10.1029/2003RG000128, 2004.

Hendy, I. L. and Kennett, J. P.: Latest Quaternary North Pacific surface-water responses imply atmosphere-driven climate instability, Geology, 27, 291–294, doi:10.1130/0091-7613(1999)027, http://geology.gsapubs.org/content/27/4/291.short, 1999.

Hu, A., Otto-Bliesner, B. L., Meehl, G. A., Han, W., Morrill, C., Brady, E. C., and Briegleb, B.: Response of Thermohaline Circulation to Freshwater Forcing under Present-Day and LGM Conditions, Journal of Climate, 21, 2239–2258, doi:10.1175/2007JCLI1985.1, http://journals.ametsoc.org/doi/abs/10.1175/2007JCLI1985.1, 2008.

Hu, A., Meehl, G. a., Han, W., Abe-Ouchi, A., Morrill, C., Okazaki, Y., and Chikamoto, M. O.: The Pacific-Atlantic seesaw and the Bering Strait, Geophysical Research Letters, 39, n/a–n/a, doi:10.1029/2011GL050567, http://doi.wiley.com/10.1029/2011GL050567, 2012.

Indermühle, A., Monnin, E., Stauffer, B., Stocker, T. F., and Wahlen, M.: Atmospheric CO 2 concentration from 60 to 20 kyr BP from the Taylor Dome Ice Core, Antarctica, Geophysical Research Letters, 27, 735–738, doi:10.1029/1999GL010960, http://doi.wiley.com/10.1029/1999GL010960, 2000.

Jaccard, S. L., Galbraith, E. D., Martínez-García, A., and Anderson, R. F.: Covariation of deep Southern Ocean oxygenation and atmospheric CO2 through the last ice age., Nature, 530, 207–210, doi:10.1038/nature16514, http://dx.doi.org/10.1038/nature16514, 2016.

Kageyama, M., Merkel, U., Otto-Bliesner, B., Prange, M., Abe-Ouchi, A., Lohmann, G., Ohgaito, R., Roche, D. M., Singarayer, J., Swingedouw, D., and X Zhang: Climatic impacts of fresh water hosing under Last Glacial Maximum conditions: a multi-model study, Climate of the Past, 9, 935–953, doi:10.5194/cp-9-935-2013, http://www.clim-past.net/9/935/2013/, 2013.

Kaspi, Y., Sayag, R., and Tziperman, E.: A "triple sea-ice state" mechanism for the abrupt warming and synchronous ice sheet collapses during Heinrich events, Paleoceanography, 19, n/a–n/a, doi:10.1029/2004PA001009, http://doi.wiley.com/10.1029/2004PA001009, 2004.

Kim, J.-H., Romero, O. E., Lohmann, G., Donner, B., Laepple, T., Haam, E., and Sinninghe Damsté, J. S.: Pronounced subsurface cooling of North Atlantic waters off Northwest Africa during Dansgaard–Oeschger interstadials, Earth and Planetary Science Letters, 339-340, 95–102, doi:10.1016/j.epsl.2012.05.018, http://www.sciencedirect.com/science/article/pii/S0012821X12002440, 2012.

Krebs, U. and Timmermann, A.: Tropical Air–Sea Interactions Accelerate the Recovery of the Atlantic Meridional Overturning Circulation after a Major Shutdown, Journal of Climate, 20, 4940–4956, doi:10.1175/JCLI4296.1, http://journals.ametsoc.org/doi/abs/10.1175/JCLI4296.1, 2007.

Laskar, J., Robutel, P., Joutel, F., Gastineau, M., Correia, a. C. M., and Levrard, B.: A long-term numerical solution for the insolation quantities of the Earth, Astronomy and Astrophysics, 428, 261–285, doi:10.1051/0004-6361:20041335, http://www.edpsciences.org/10.1051/0004-6361:20041335, 2004.

Li, C.: Abrupt climate shifts in Greenland due to displacements of the sea ice edge, Geophysical Research Letters, 32, L19 702, doi:10.1029/2005GL023492, http://doi.wiley.com/10.1029/2005GL023492, 2005.

Li, C., Battisti, D. S., and Bitz, C. M.: Can North Atlantic Sea Ice Anomalies Account for Dansgaard–Oeschger Climate Signals?*, Journal of Climate, 23, 5457–5475, doi:10.1175/2010JCLI3409.1, http://journals.ametsoc.org/doi/abs/10.1175/2010JCLI3409.1, 2010.

Liu, Z., Otto-Bliesner, B. L., He, F., Brady, E. C., Tomas, R., Clark, P. U., Carlson, A. E., Lynch-Stieglitz, J., Curry, W., Brook, E., Erickson, D., Jacob, R., Kutzbach, J., and Cheng, J.: Transient simulation of last deglaciation with a new mechanism for Bolling-Allerod warming., Science (New York, N.Y.), 325, 310–4, doi:10.1126/science.1171041, http://www.sciencemag.org/content/325/5938/310.abstract, 2009.

Loving, J. L. and Vallis, G. K.: Mechanisms for climate variability during glacial and interglacial periods, Paleoceanography, 20, n/a–n/a, doi:10.1029/2004PA001113, http://doi.wiley.com/10.1029/2004PA001113, 2005.

Luthi, D., Le Floch, M., Bereiter, B., Blunier, T., Barnola, J.-M., Siegenthaler, U., Raynaud, D., Jouzel, J., Fischer, H., Kawamura, K., and Stocker, T. F.: High-resolution carbon dioxide concentration record 650,000-800,000[thinsp]years before present, Nature, 453, 379–382, http://dx.doi.org/10.1038/nature06949http://www.nature.com/nature/journal/v453/n7193/suppinfo/nature06949{_}S1.html, 2008.

MacAyeal, D. R.: Binge/purge oscillations of the Laurentide Ice Sheet as a cause of the North Atlantic's Heinrich events, Paleoceanography, 8, 775–784, doi:10.1029/93PA02200, http://doi.wiley.com/10.1029/93PA02200, 1993.

Marcott, S. a., Clark, P. U., Padman, L., Klinkhammer, G. P., Springer, S. R., Liu, Z., Otto-Bliesner, B. L., Carlson, A. E., Ungerer, A., Padman, J., He, F., Cheng, J., and Schmittner, A.: Ice-shelf collapse from subsurface warming as a trigger for Heinrich events., Proceedings of the National Academy of Sciences of the United States of America, 108, 13 415–9, doi:10.1073/pnas.1104772108, http://www.pubmedcentral.nih.gov/articlerender.fcgi?artid=3158189{&}tool=pmcentrez{&}rendertype=abstract, 2011.

Mariotti, V., Bopp, L., Tagliabue, a., Kageyama, M., and Swingedouw, D.: Marine productivity response to Heinrich events: a model-data comparison, Climate of the Past, 8, 1581–1598, doi:10.5194/cp-8-1581-2012, http://www.clim-past.net/8/1581/2012/, 2012.

Marshall, S. J. and Koutnik, M. R.: Ice sheet action versus reaction: Distinguishing between Heinrich events and Dansgaard-Oeschger cycles in the North Atlantic, Paleoceanography, 21, PA2021, doi:10.1029/2005PA001247, http://doi.wiley.com/10.1029/2005PA001247, 2006.

Menviel, L., Timmermann, a., Friedrich, T., and England, M. H.: Hindcasting the continuum of Dansgaard–Oeschger variability: mechanisms, patterns and timing, Climate of the Past, 10, 63–77, doi:10.5194/cp-10-63-2014, http://www.clim-past.net/10/63/2014/, 2014.

Mignot, J., Ganopolski, A., and Levermann, A.: Atlantic Subsurface Temperatures: Response to a Shutdown of the Overturning Circulation and Consequences for Its Recovery, Journal of Climate, 20, 4884–4898, doi:10.1175/JCLI4280.1, http://journals.ametsoc.org/doi/abs/10.1175/jcli4280.1, 2007.

Okazaki, Y., Timmermann, a., Menviel, L., Harada, N., Abe-Ouchi, a., Chikamoto, M. O., Mouchet, a., and Asahi, H.: Deepwater formation in the North Pacific during the Last Glacial Termination., Science (New York, N.Y.), 329, 200–4, doi:10.1126/science.1190612, http://www.ncbi.nlm.nih.gov/pubmed/20616275, 2010.

Okumura, Y. M., Deser, C., Hu, A., Timmermann, A., and Xie, S.-P.: North Pacific Climate Response to Freshwater Forcing in the Subarctic North Atlantic: Oceanic and Atmospheric Pathways, Journal of Climate, 22, 1424–1445, doi:10.1175/2008JCLI2511.1, http://dx.doi.org/10.1175/2008JCLI2511.1, 2009.

Otto-Bliesner, B. L. and Brady, E. C.: The sensitivity of the climate response to the magnitude and location of freshwater forcing: last glacial maximum experiments, Quaternary Science Reviews, 29, 56–73, doi:10.1016/j.quascirev.2009.07.004, http://www.sciencedirect.com/science/article/pii/S0277379109002340, 2010.

Palter, J. B., Griffies, S. M., Samuels, B. L., Galbraith, E. D., Gnanadesikan, A., and Klocker, A.: The Deep Ocean Buoyancy Budget and Its Temporal Variability, Journal of Climate, 27, 551–573, doi:10.1175/JCLI-D-13-00016.1, http://journals.ametsoc.org/doi/abs/10.1175/JCLI-D-13-00016.1, 2014.

Pausata, F. S. R., Grini, A., Caballero, R., Hannachi, A., and Seland, Ø.: High-latitude volcanic eruptions in the Norwegian Earth System Model: the effect of different initial conditions and of the ensemble size, Tellus B, 67, doi:10.3402/tellusb.v67.26728, http://www.tellusb.net/index.php/tellusb/article/view/26728/xml{_}15, 2015.

Peltier, W. R. and Vettoretti, G.: Dansgaard-Oeschger oscillations predicted in a comprehensive model of glacial climate: A “kicked” salt oscillator in the Atlantic, Geophysical Research Letters, 41, 7306–7313, doi:10.1002/2014GL061413, http://doi.wiley.com/10.1002/2014GL061413, 2014.

Petersen, S. V., Schrag, D. P., and Clark, P. U.: A new mechanism for Dansgaard-Oeschger cycles, Paleoceanography, 28, 24–30, doi:10.1029/2012PA002364, http://doi.wiley.com/10.1029/2012PA002364, 2013.

Peterson, L. C.: Rapid Changes in the Hydrologic Cycle of the Tropical Atlantic During the Last Glacial, Science, 290, 1947–1951, doi:10.1126/science.290.5498.1947, http://science.sciencemag.org/content/290/5498/1947.abstract, 2000.

Rahmstorf, S., Crucifix, M., Ganopolski, A., Goosse, H., Kamenkovich, I., Knutti, R., Lohmann, G., Marsh, R., Mysak, L. A., Wang, Z., and Weaver, A. J.: Thermohaline circulation hysteresis: A model intercomparison, Geophysical Research Letters, 32, L23 605, doi:10.1029/2005GL023655, http://doi.wiley.com/10.1029/2005GL023655, 2005.

Roberts, W. H. G., Valdes, P. J., and Payne, A. J.: Topography's crucial role in Heinrich Events., Proceedings of the National Academy of Sciences of the United States of America, 111, 16 688–93, doi:10.1073/pnas.1414882111, http://www.pnas.org/content/111/47/16688.short, 2014.

Roche, D. M., Renssen, H., Weber, S. L., and Goosse, H.: Could meltwater pulses have been sneaked unnoticed into the deep ocean during the last glacial?, Geophysical Research Letters, 34, L24 708, doi:10.1029/2007GL032064, http://doi.wiley.com/10.1029/2007GL032064, 2007.

Rooth, C.: Hydrology and ocean circulation, Progress in Oceanography, 11, 131–149, 1982.

Saenko, O. A., Schmittner, A., and Weaver, A. J.: The Atlantic – Pacific Seesaw, Journal of Climate, 17, 2033–2038, 2004.

Sakai, K. and Peltier, W. R.: Dansgaard–Oeschger Oscillations in a Coupled Atmosphere–Ocean Climate Model, Journal of Climate, 10, 949–970, doi:10.1175/1520-0442(1997)010<0949:DOOIAC>2.0.CO;2, http://dx.doi.org/10.1175/1520-0442(1997)010<0949:DOOIAC>2.0.CO2, 1997.

Sarmiento, J. L. and Toggweiler, J. R.: A new model for the role of the oceans in determining atmospheric PCO2, Nature, 308, 621–624, doi:10.1038/308621a0, http://dx.doi.org/10.1038/308621a0, 1984.

Schmidt, M. W., Vautravers, M. J., and Spero, H. J.: Rapid subtropical North Atlantic salinity oscillations across Dansgaard-Oeschger cycles., Nature, 443, 561–4, doi:10.1038/nature05121, http://dx.doi.org/10.1038/nature05121, 2006.

Schmittner, A.: Decline of the marine ecosystem caused by a reduction in the Atlantic overturning circulation., Nature, 434, 628–33, doi:10.1038/nature03476, http://dx.doi.org/10.1038/nature03476, 2005.

Schmittner, A. and Galbraith, E. D.: Glacial greenhouse-gas fluctuations controlled by ocean circulation changes., Nature, 456, 373–6, doi:10.1038/nature07531, http://dx.doi.org/10.1038/nature07531, 2008.

Schmittner, A., Yoshimori, M., and Weaver, A. J.: Instability of glacial climate in a model of the ocean-atmosphere-cryosphere system., Science (New York, N.Y.), 295, 1489–93, doi:10.1126/science.1066174, http://science.sciencemag.org/content/295/5559/1489.abstract, 2002.

Schmittner, A., Brooke, E., and Ahn, J.: Ocean Circulation: Mechanisms and Impacts, vol. 173, chap, Impact of the ocean's overturning circulation on atmospheric CO2, AGU Geophysical Monograph Series, pp. 209–246, 2007a.

Schmittner, A., Galbraith, E. D., Hostetler, S. W., Pedersen, T. F., and Zhang, R.: Large fluctuations of dissolved oxygen in the Indian and Pacific oceans during Dansgaard-Oeschger oscillations caused by variations of North Atlantic Deep Water subduction, Paleoceanography, 22, n/a–n/a, doi:10.1029/2006PA001384, http://doi.wiley.com/10.1029/2006PA001384, 2007b.

Schulz, M.: Relaxation oscillators in concert: A framework for climate change at millennial timescales during the late Pleistocene, Geophysical Research Letters, 29, 2193, doi:10.1029/2002GL016144, http://doi.wiley.com/10.1029/2002GL016144, 2002.

Shaffer, G.: Ocean subsurface warming as a mechanism for coupling Dansgaard-Oeschger climate cycles and ice-rafting events, Geophysical Research Letters, 31, L24 202, doi:10.1029/2004GL020968, http://doi.wiley.com/10.1029/2004GL020968, 2004.

Siddall, M., Rohling, E. J., Blunier, T., and Spahni, R.: Patterns of millennial variability over the last 500 ka, Climate of the Past, 6, 295–303, doi:10.5194/cp-6-295-2010, http://www.clim-past.net/6/295/2010/cp-6-295-2010.html, 2010.

Sigman, D. M., Hain, M. P., and Haug, G. H.: The polar ocean and glacial cycles in atmospheric CO(2) concentration., Nature, 466, 47–55, doi:10.1038/nature09149, http://dx.doi.org/10.1038/nature09149, 2010.

Stocker, T. F. and Johnsen, S. J.: A minimum thermodynamic model for the bipolar seesaw, Paleoceanography, 18, n/a–n/a, doi:10.1029/2003PA000920, http://doi.wiley.com/10.1029/2003PA000920, 2003.

Stommel, H.: Thermohaline Convection with Two Stable Regimes of Flow, Tellus, 13, 224–230, doi:10.1111/j.2153-3490.1961.tb00079.x, http://dx.doi.org/10.1111/j.2153-3490.1961.tb00079.x, 1961.

Stouffer, R. J., Yin, J., Gregory, J. M., Dixon, K. W., Spelman, M. J., Hurlin, W., Weaver, A. J., Eby, M., Flato, G. M., Hasumi, H., Hu, A., Jungclaus, J. H., Kamenkovich, I. V., Levermann, A., Montoya, M., Murakami, S., Nawrath, S., Oka, A., Peltier, W. R., Robitaille, D. Y., Sokolov, A., Vettoretti, G., and Weber, S. L.: Investigating the Causes of the Response of the Thermohaline Circulation to Past and Future Climate Changes, Journal of Climate, 19, 1365–1387, doi:10.1175/JCLI3689.1, http://dx.doi.org/10.1175/JCLI3689.1, 2006.

Tarasov, L. and Peltier, W. R.: Arctic freshwater forcing of the Younger Dryas cold reversal., Nature, 435, 662–5, doi:10.1038/nature03617, http://dx.doi.org/10.1038/nature03617, 2005.

Timmermann, A., Gildor, H., Schulz, M., and Tziperman, E.: Coherent Resonant Millennial-Scale Climate Oscillations Triggered by Massive Meltwater Pulses, Journal of Climate, 16, 2569–2585, doi:10.1175/1520-0442(2003)016<2569:CRMCOT>2.0.CO;2, http://journals.ametsoc.org/doi/abs/10.1175/1520-0442(2003)016{%}3C2569{%}3ACRMCOT{%}3E2.0.CO{%}3B2, 2003.

Vettoretti, G. and Peltier, W. R.: Interhemispheric air temperature phase relationships in the nonlinear Dansgaard-Oeschger oscillation, Geophysical Research Letters, 42, 1180–1189, doi:10.1002/2014GL062898, http://doi.wiley.com/10.1002/2014GL062898, 2015.

Voelker, A. H.: Global distribution of centennial-scale records for Marine Isotope Stage (MIS) 3: a database, Quaternary Science Reviews, 21, 1185–1212, doi:10.1016/S0277-3791(01)00139-1, http://www.sciencedirect.com/science/article/pii/S0277379101001391, 2002.

Wang, X., Auler, A. S., Edwards, R. L., Cheng, H., Cristalli, P. S., Smart, P. L., Richards, D. A., and Shen, C.-C.: Wet periods in northeastern Brazil over the past 210 kyr linked to distant climate anomalies., Nature, 432, 740–3, doi:10.1038/nature03067, http://dx.doi.org/10.1038/nature03067, 2004.

Wang, Y. J., Cheng, H., Edwards, R. L., An, Z. S., Wu, J. Y., Shen, C. C., and Dorale, J. A.: A high-resolution absolute-dated late Pleistocene Monsoon record from Hulu Cave, China., Science (New York, N.Y.), 294, 2345–8, doi:10.1126/science.1064618, http://science.sciencemag.org/content/294/5550/2345.abstract, 2001.

Wang, Z. and Mysak, L. a.: Glacial abrupt climate changes and Dansgaard-Oeschger oscillations in a coupled climate model, Paleoceanography, 21, 1–9, doi:10.1029/2005PA001238, 2006.

Weaver, A. J. and Sarachik, E. S.: The Role of Mixed Boundary Conditions in Numerical Models of the Ocean's Climate, Journal of Physical Oceanography, 21, 1470–1493, doi:10.1175/1520-

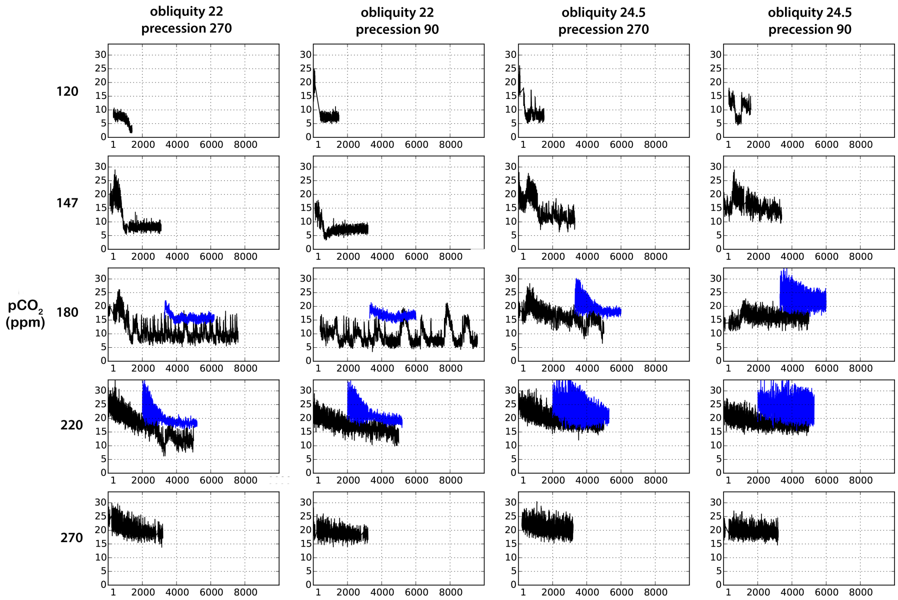

Figure 1. Timeseries of AMOC for the matrix of simulations with prescribed atmospheric pCO_2 (rows) and orbital configurations (columns). Black lines have preindustrial ice-sheets and blue lines, when applicable, have full LGM ice-sheets. The AMOC, shown on the vertical axes in Sverdrups, is defined as maximum of Atlantic meridional stream function between 30N:50N and water depths of 500:5000m. Precessional phases of 270°and 90°are equivalent to strong and weak boreal seasonalities, respectively.

0485(1991)021<1470:TROMBC>2.0.CO;2, http://journals.ametsoc.org/doi/abs/10.1175/1520-0485(1991)021{%}3C1470:TROMBC{%}3E2.0.CO{%}3B2, 1991.

Weaver, A. J., Saenko, O. A., Clark, P. U., and Mitrovica, J. X.: Meltwater pulse 1A from Antarctica as a trigger of the Bølling-Allerød warm interval., Science (New York, N.Y.), 299, 1709–13, doi:10.1126/science.1081002, http://science.sciencemag.org/content/299/5613/1709.abstract, 2003.

Winton, M.: Deep Decoupling Oscillations of the Oceanic Thermohaline Circulation, 1993.

Zhang, X., Lohmann, G., Knorr, G., and Purcell, C.: Abrupt glacial climate shifts controlled by ice sheet changes, Nature, 512, 290–294, doi:10.1038/nature13592, http://dx.doi.org/10.1038/nature13592, 2014.

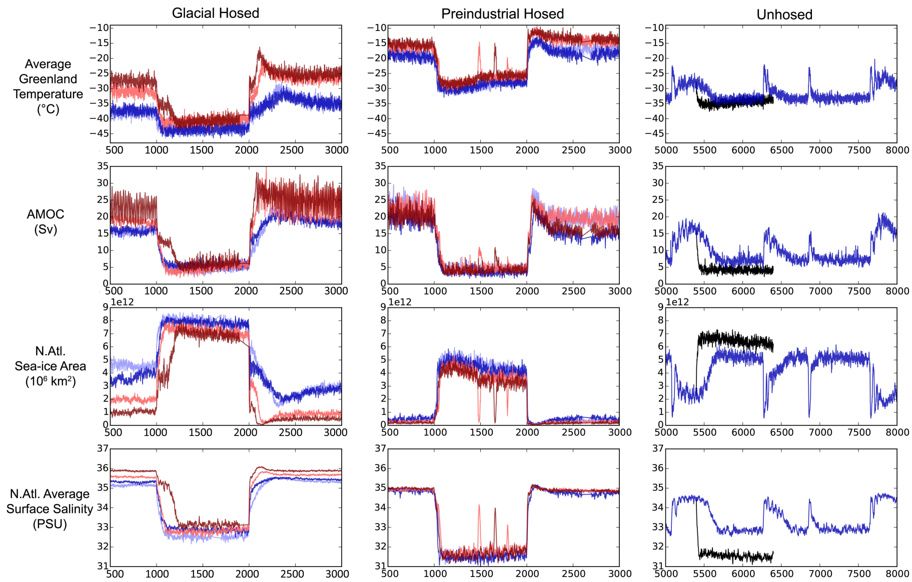

Figure 2. North Atlantic climate metrics for all simulations. The left column shows four simulations under the Glacial boundary conditions (LGM ice sheets and bathymetry with closed Bering Strait; 180 ppm CO_2), the central column shows four simulations run under the Preindustrial boundary conditions (Preindustrial ice sheets and bathymetry; 270 ppm CO_2), and the right column shows the Unhosed simulation in which spontaneous AMOC variations occur under constant boundary conditions. For the left and center columns, freshwater hosing was applied between years 1001 and 2000. Orbital configurations are indicated as follows: red=high obliquity; blue=low obliquity; dark=weak boreal seasonality; pale=strong boreal seasonality. The black lines in the right column show the 'Hosed-Unhosed' simulation, in which 0.2 Sv of freshwater was added in the North Atlantic during an unforced AMOC 'interstadial'. AMOC is defined as the maximum Atlantic streamfunction between 500m-5500m and 30N:50N.

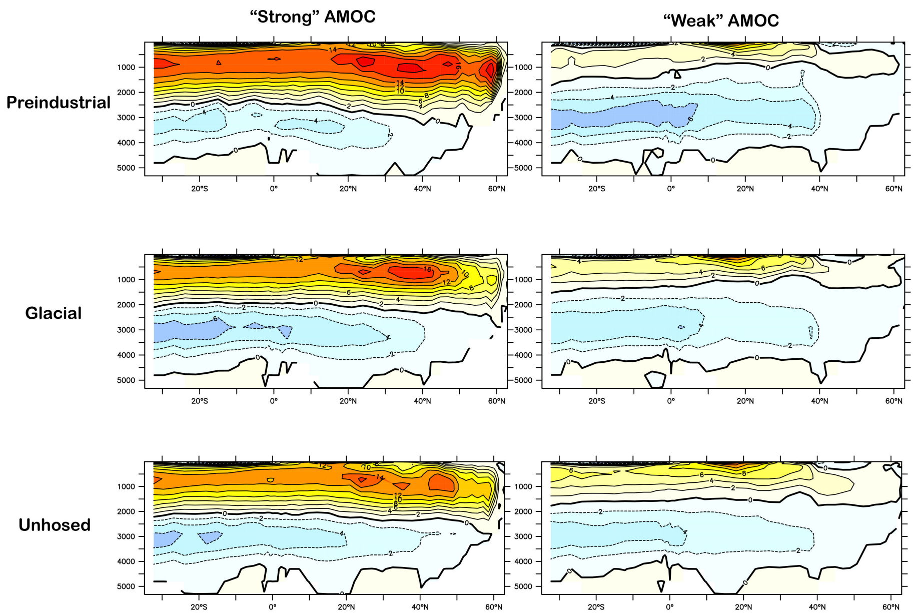

Figure 3. Atlantic meridional overturning streamfunctions in strong and weak states. All plots show 100-year averages. In Glacial and Preindustrial hosing simulations, weak AMOC state is defined by averaging the last century of hosing (model years 1901-2000) and strong AMOC state is defined by averaging the same years from the corresponding control simulation (to correct for potential drift). In the Unhosed simulation, the weak AMOC state is defined by averaging model years 7501-7600 and the strong AMOC state is defined by averaging model years 7901-8000. For the top two rows, the streamfunctions are averaged over the corresponding four sets of orbital configurations. The bottom row shows the streamfunctions for the Unhosed simulation. Contours in Sverdrups.

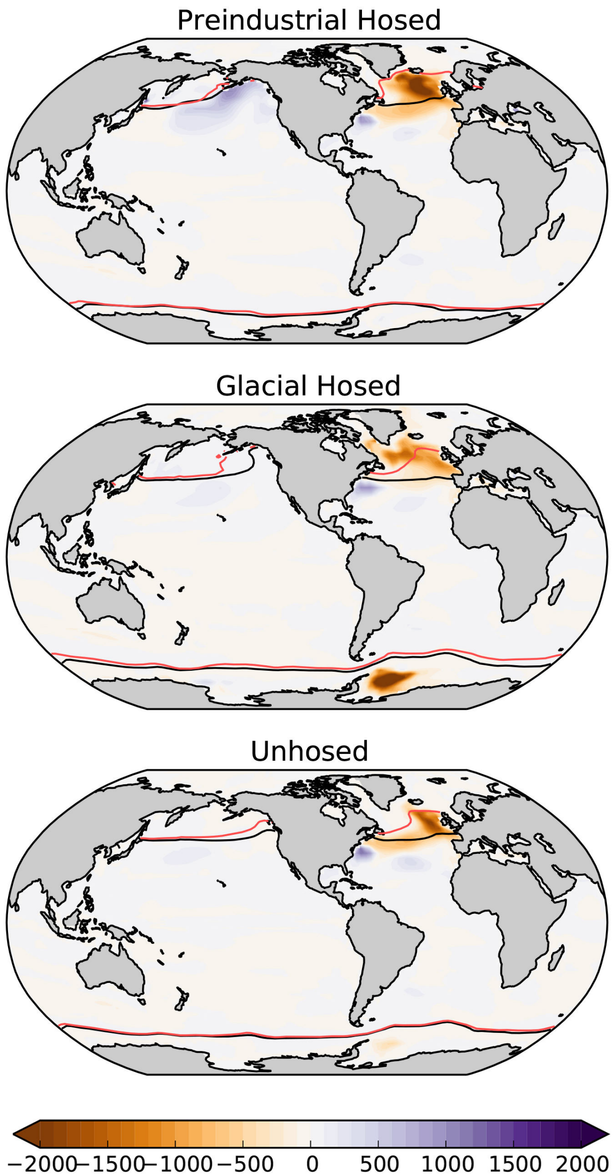

Figure 4. Stadial winter mixed-layer depth anomaly. The top two panels show the difference in winter mixed-layer depth between weak and strong AMOC states (as defined in Fig.3) under Preindustrial and Glacial boundary conditions, averaged between the four sets of orbital configurations (see Supplementary Figure 1 to view all 8 hosing simulations individually). The bottom panel shows the winter mixed-layer depth between weak and strong AMOC states (as defined in Fig.3) in the Unhosed simulation. Black and red contours show the sea-ice edge for the weak AMOC and strong AMOC states, respectively. Sea-ice edge is defined as >30% of annually-averaged ice concentration. Shading in m.

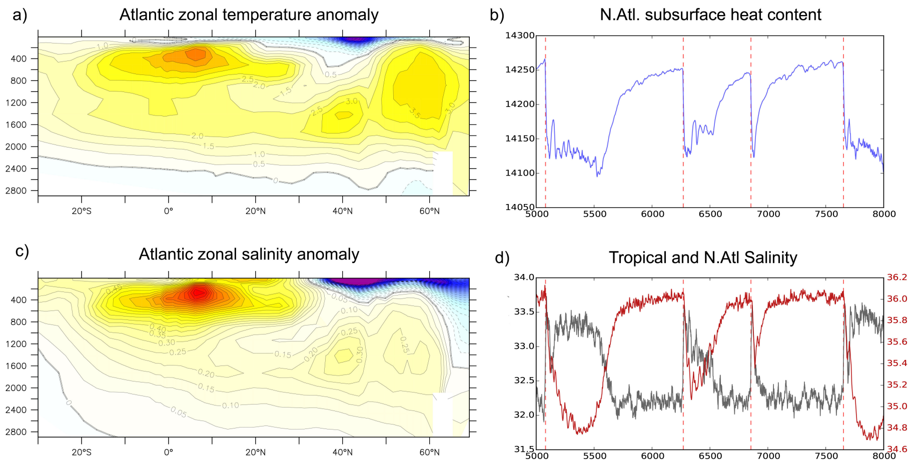

Figure 5. Thermohaline oscillations in the Unhosed simulation. a,c) Atlantic zonally-averaged temperature/salinity anomaly between weak AMOC (years 7501-7600) state and strong AMOC state (years 7901-8000). Units in °C / PSU. b) Subsurface (500-2500m) heat content in the North Atlantic (>45°N). Units in ZettaJoules. d) Sea surface salinity in the North Atlantic (>45°N) (black) and Tropical Atlantic (0:10 °N, 70:30 °W) (red). Units in PSU. Red vertical dashed lines indicate onset of deep convection in the North Atlantic.

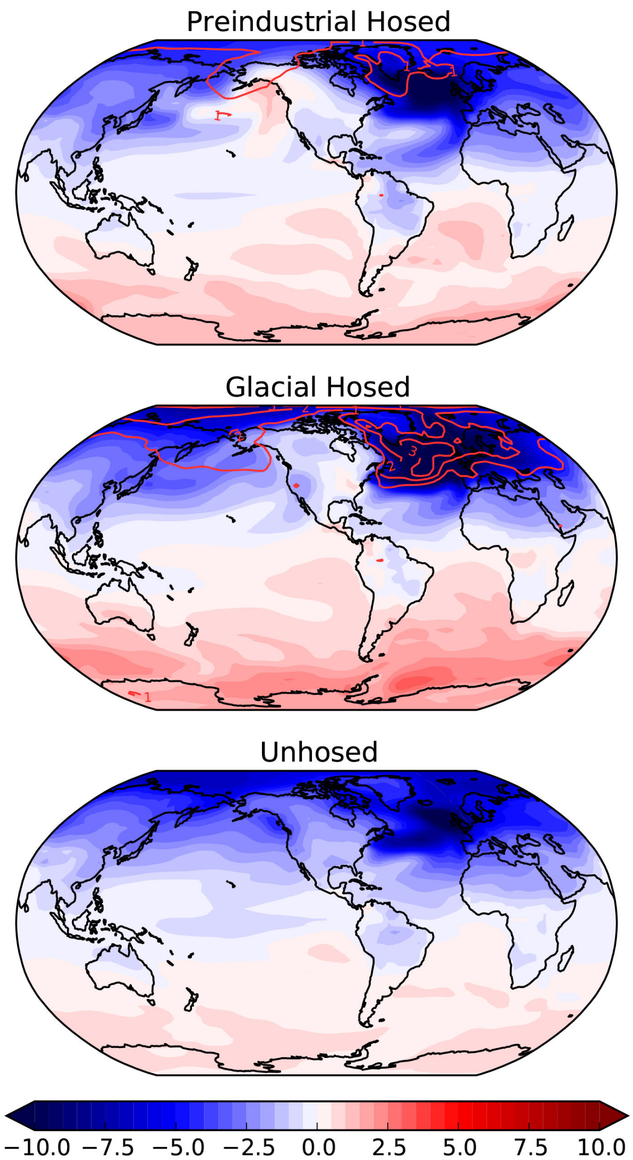

Figure 6. Stadial surface air temperature anomaly. The top two panels show the surface air temperature difference between weak and strong AMOC states (as defined in Fig.3) under Preindustrial and Glacial boundary conditions, averaged between the four sets of orbital configurations (see Supplementary Figure 2 to view all 8 hosing simulations individually). Red contours show the standard deviation between the four sets of orbital configurations at 1°C intervals. The bottom panel shows the surface air temperature difference between weak and strong AMOC states (as defined in Fig.3) in the Unhosed simulation. Shading and contours in °C.

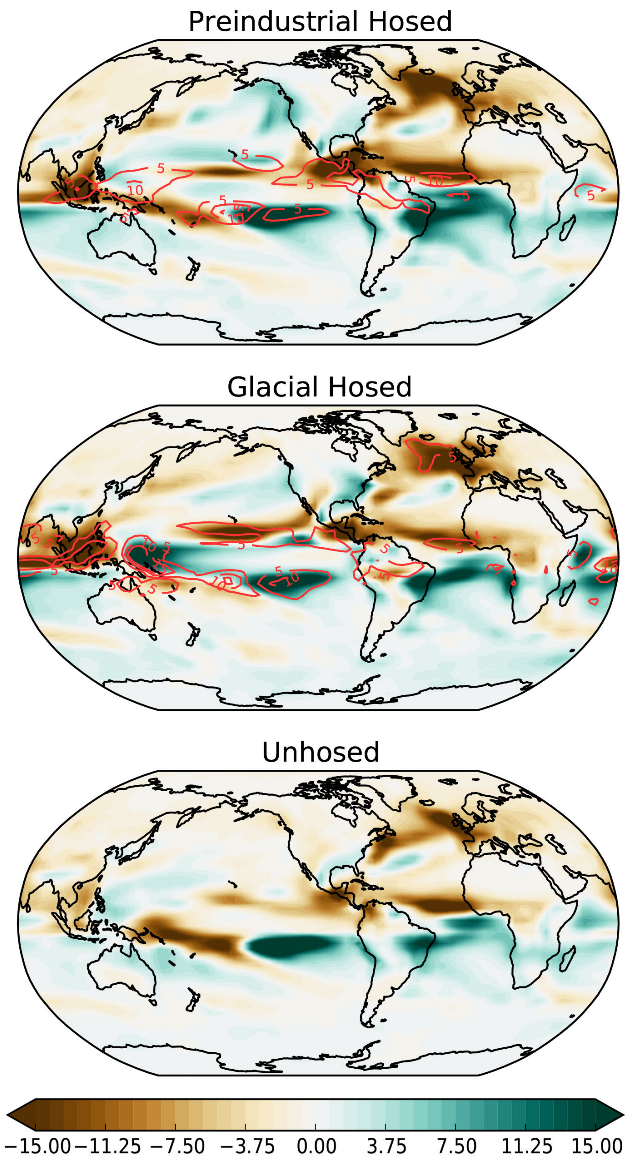

Figure 7. Stadial precipitation anomaly. The top two panels show the precipitation difference between weak and strong AMOC states (as defined in Fig.3) under Preindustrial and Glacial boundary conditions, averaged between the four sets of orbital configurations (see Supplementary Figure 3 to view all 8 hosing simulations individually). Red contours show the standard deviation between the four sets of orbital configurations at 5 x 10^{-6} kg m^{-2} s^{-1} intervals. The bottom panel shows the precipitation difference between weak and strong AMOC states (as defined in Fig.3) in the Unhosed simulation. Shading and contours in 10^{-6} kg m^{-2} s^{-1}.

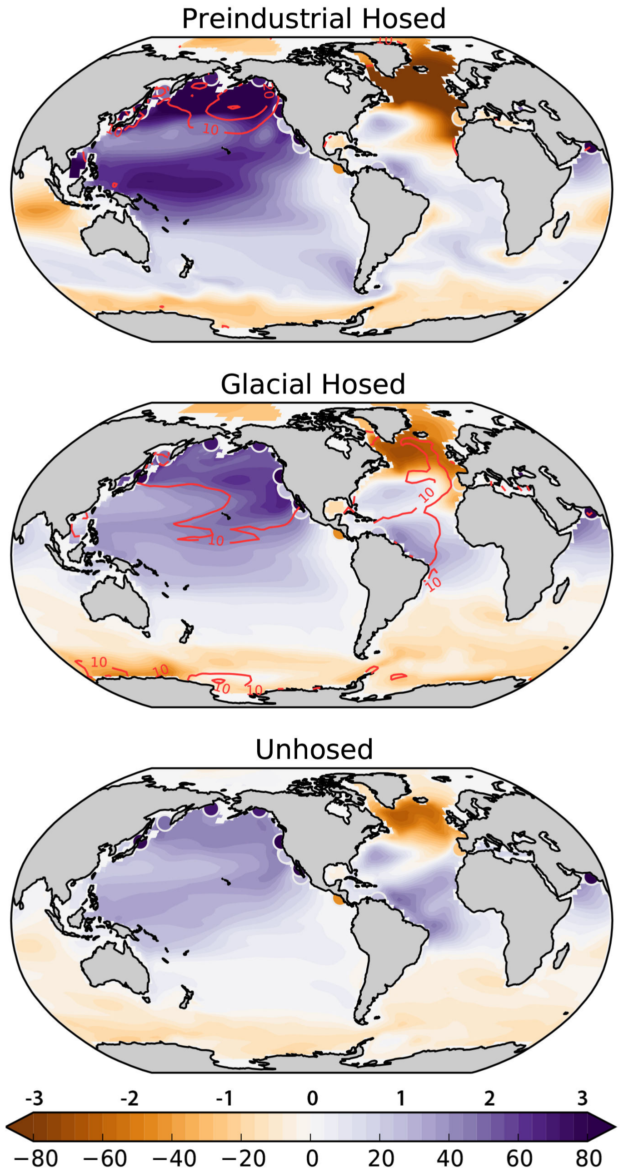

Figure 8. Stadial intermediate-depth (400m-1100m) oxygen concentration anomaly. The top two panels show the oxygen concentration difference between weak and strong AMOC states (as defined in Fig.3) under Preindustrial and Glacial boundary conditions, averaged between the four sets of orbital configurations (see Supplementary Figure 4 to view all 8 hosing simulations individually). Red contours show the standard deviation between the four sets of orbital configurations at μmol kg^{-1} intervals. The bottom panel shows the oxygen concentration difference between weak and strong AMOC states (as defined in Fig.3) in the Unhosed simulation. Markers represent the 1st principal component of the detrended time series for benthic oxygenation proxies compiled by Galbraith and Jaccard (2015). Shading and contours in μmol kg^{-1}.

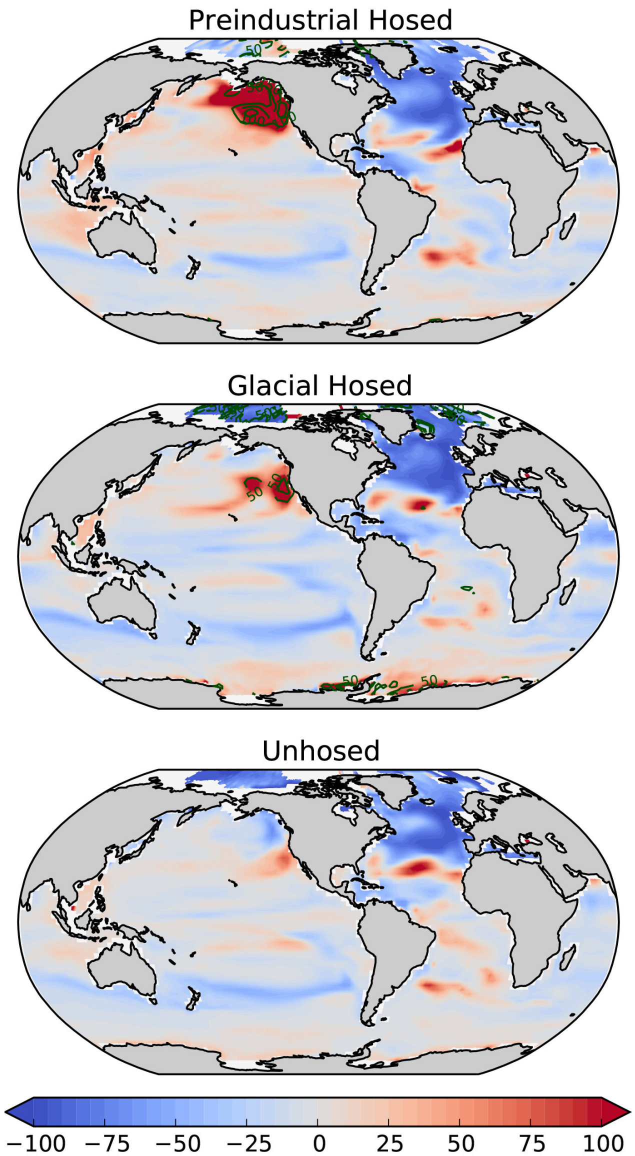

Figure 9. Stadial export production anomaly. The top two panels show the ratio of organic matter export at 100m between weak and strong AMOC states (as defined in Fig.3) under Preindustrial and Glacial boundary conditions, averaged between the four sets of orbital configurations (see Supplementary Figure 5 to view all 8 hosing simulations individually). Green contours show the standard deviation between the four sets of orbital configurations at 50 % intervals. The bottom panel shows the ratio of export between weak and strong AMOC states (as defined in Fig.3) in the Unhosed simulation. Shading and contours in %.

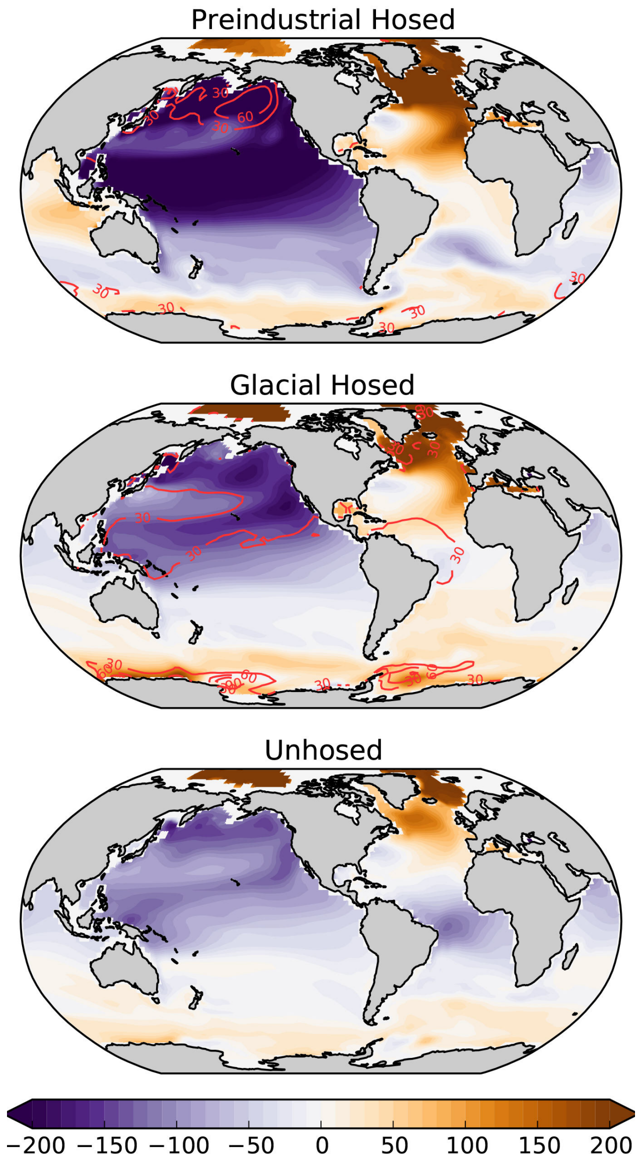

Figure 10. Stadial intermediate-depth (400m-1100m) ideal age anomaly. The top two panels show the age difference between weak and strong AMOC states (as defined in Fig.3) under Preindustrial and Glacial boundary conditions, averaged between the four sets of orbital configurations (see Supplementary Figure 6 to view all 8 hosing simulations individually). Red contours show the standard deviation between the four sets of orbital configurations at 30 year intervals. The bottom panel shows the age difference between weak and strong AMOC states (as defined in Fig.3) in the Unhosed simulation. Shading and contours in years.

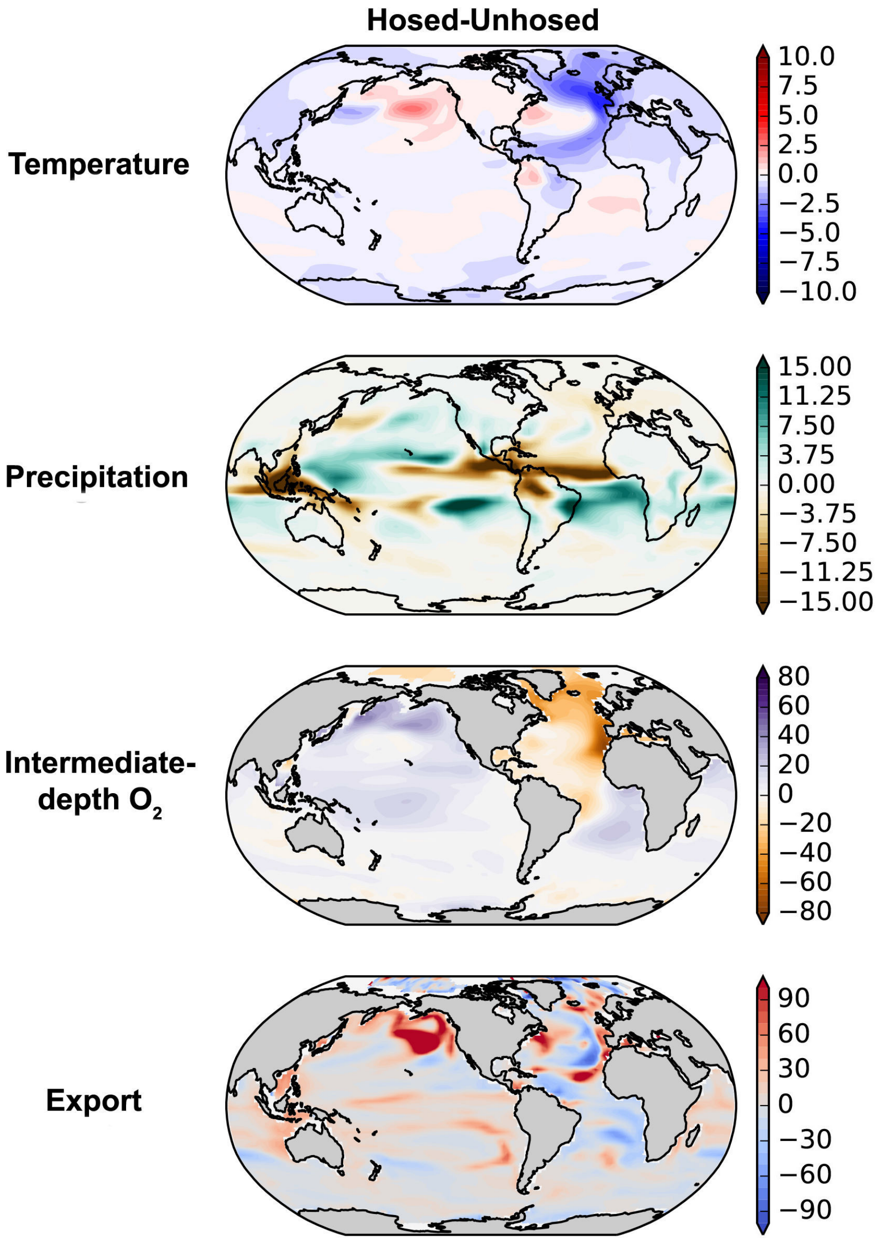

Figure 11. Impacts of hosing the Unhosed. Differences between the last century (model years 6151-6250) of the 800-year hosed-Unhosed stadial and the corresponding unhosed stadial. Scale and units are the same as in figures 6,7,8, and 9.